



A DUAL ISOLATION SYSTEM FOR ACHIEVING REDUCED DEMAND PARAMETERS

Ashkan Ezazi

Master's Candidate, McMaster University, Canada
ezazia@mcmaster.ca

Tracy C. Becker

Assistant Professor, McMaster University, Canada
tbecker@mcmaster.ca

ABSTRACT: Base isolated buildings experience enhanced performance due to minimized accelerations as well as decreased story drifts. However, the reduced demands are obtained at the expense of large displacements. This study suggests a new system, which retains the base level isolation layer and incorporates an additional isolation layer mid-story. This system, termed “dual isolation”, is comparable to the use of a tuned mass damper with a significantly larger than normal mass ratio. Response spectrum analysis is used to investigate the optimal design of this system including selection of isolation periods, mass ratio, and damping values. Time history responses of the dual isolation system are compared to those of a conventional base isolation counterpart to examine the effectiveness of the system. The dual isolation system reduces the floor acceleration of the upper portion of the building significantly compared to the accelerations in a classic base isolated building. In addition, the displacement of the first level of isolation is reduced by up to 48%.

1. Introduction

Classical isolated buildings experience minimized floor accelerations and interstory drifts compared to fixed base buildings under seismic excitations. However, there is a trade-off between reduced transmitted acceleration and the large displacement demand at the interface of isolation layer. To accommodate this large displacement, designers must provide large isolation gaps, which increases the total project cost. The most common approach for decreasing displacements in isolation systems is to incorporate supplementary damping to the system. Although controlling the isolator displacement by additional damping is effective, it can increase floor acceleration and story drifts in the superstructure through excitation of higher modes (Kelly, 1999). Wolff et al. (2015) showed that for low damped bearings the addition of damper devices results in reduction in displacement demand without having detrimental effect on floor acceleration and story drifts, however for highly damped isolation systems (effective damping of 20-30%) the addition of damper devices leads to a general increase in drifts and shear forces of base isolated buildings. Furthermore, supplementary hysteretic damping can limit the isolation system's ability to displace during lower level earthquakes.

The effectiveness of tuned mass dampers (TMDs) on the seismic behaviour of fixed base buildings has been investigated in many studies. TMDs have been found to have limited effectiveness, highly dependent on the ground motion properties (Chowdhury and Iwuchkw, 1987, Clark, 1988, Sladek and Klinger, 1983, Matta 2013). Studies on seismic behaviour of base isolated buildings equipped with TMDs show similar trends. Palazzo and Petti (1999) and Taniguchi et al. (2008) investigated the performance of a base isolated system with TMDs added to control the displacement demand. Taniguchi et al. (2008) showed that TMDs located directly above the isolation layer can reduce the displacement demand of lightly damped (below 10%) base-isolated structures by up to 25% for white noise and far field excitations.

However, both studies found that the TMD efficacy decreases as the damping ratio of the isolators increases.

Chien Pan et al. (1995) introduced the concept of multi-layer isolation (more than two layers) to improve the effectiveness of base isolation in tall buildings. They numerically investigated a 16 story structure divided into four segments under the El Centro ground motion and observed a 37% decrease in base displacement while maintaining structural accelerations similar to a classic base isolated case. Ryan and Earl (2010) studied the displacement demand in a six story building with multiple isolation layers varying the locations of the isolation systems. Numerical results showed roughly 30% reduction in base displacement and 30% increase in roof displacement in the system with two isolation layers located at the base and mid-height compared to a classic base isolated model. However, the location and properties of the isolation layers were not optimized, and the potential for reducing floor accelerations was not considered.

The presented study aims to reduce the displacement of the base isolation level by applying an additional layer of isolation mid-story. The combined system is referred to as 'dual isolation.' Using simplified models, the performance of the dual isolation system is compared to classic base isolation under a suite of ground motions including broadband and pulse type motions. In addition, the effect of the system properties including mass ratio, and damping ratios of the isolation layers are investigated by response spectrum analysis to find an optimal state for the system in design practices. Lastly, the two degree of freedom (DOF) model is extended to a multi DOF model to explore the effect of higher modes on interstory drifts and floor response spectra.

2. Response Spectrum Analysis

2.1. Dual Isolation Model

The theory for the dual isolation system is based on classic linear isolation theory, given in Naeim and Kelly (1999). This theory is based on a two degree of freedom (DOF) structural model with one DOF representing the isolation layer with period T_1 and damping ratio of β_1 and the second DOF representing the superstructure with period T_2 and damping ratio of β_2 . This model considers the superstructure as an independent degree of freedom; however, the system can be estimated by a simpler analysis by treating the superstructure as rigid. The relative deformation of the superstructure is negligible when the period of the isolation system is much longer than the period of its superstructure; therefore, the combined behaviour of isolation layer and its superstructure can be considered as one DOF with period of T_1 and damping ratio of β_1 . Using this assumption, the two DOF formulation can be extended to the dual isolation system, in which each superstructure behaves as approximately rigid as shown in Fig. 1.

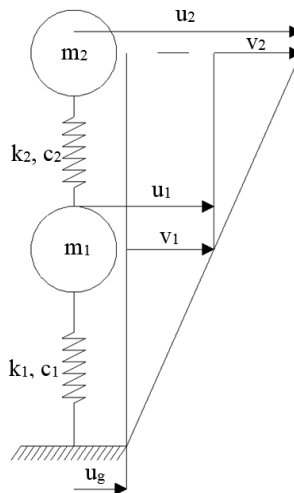


Fig. 1 - Dual Isolation Model

In Fig.1, m , k and c represent the mass, effective stiffness and viscous damping coefficient of each isolation system, and v_1 , v_2 and u_g shows the interstory drift of the first and second isolation systems and ground displacement respectively.

The behaviour of dual isolation system depends on its nominal frequencies ω_1 , ω_2 mass ratio γ , the frequency ratio, and damping ratios β_1 and β_2 . These parameters are defined as

$$\omega_1 = \sqrt{k_1 / (m_1 + m_2)}, \omega_2 = \sqrt{k_2 / m_2} \quad (1)$$

$$\beta_1 = \frac{c_1}{2(m_1 + m_2)\omega_1}, \beta_2 = \frac{c_2}{2m_2\omega_2} \quad (2)$$

$$\gamma = \frac{m_2}{(m_1 + m_2)} \quad (3)$$

The model presented in Fig. 1 used for a numerical response spectrum studies with a design basis earthquake (DBE) which is shown in Fig. 3. The spectrum is defined for 10% probability of exceedance in 50 years downtown Seattle, WA, USA (47.60, -122.34), (ASCE 07, 2010).

2.2. System's Behaviour

The model shown in Fig. 1 is used to investigate the behaviour of the dual isolation system. Figure 2 shows the lateral displacements of the first and second isolation systems when the nominal period of the first isolation layer T_1 is 3.5 s. Figure 2a varies the mass ratio, γ , while the equivalent viscous damping ratio of the first and second isolation layers, β_1 and β_2 are both 15%. Figure 2b varies β_1 , while β_2 is kept

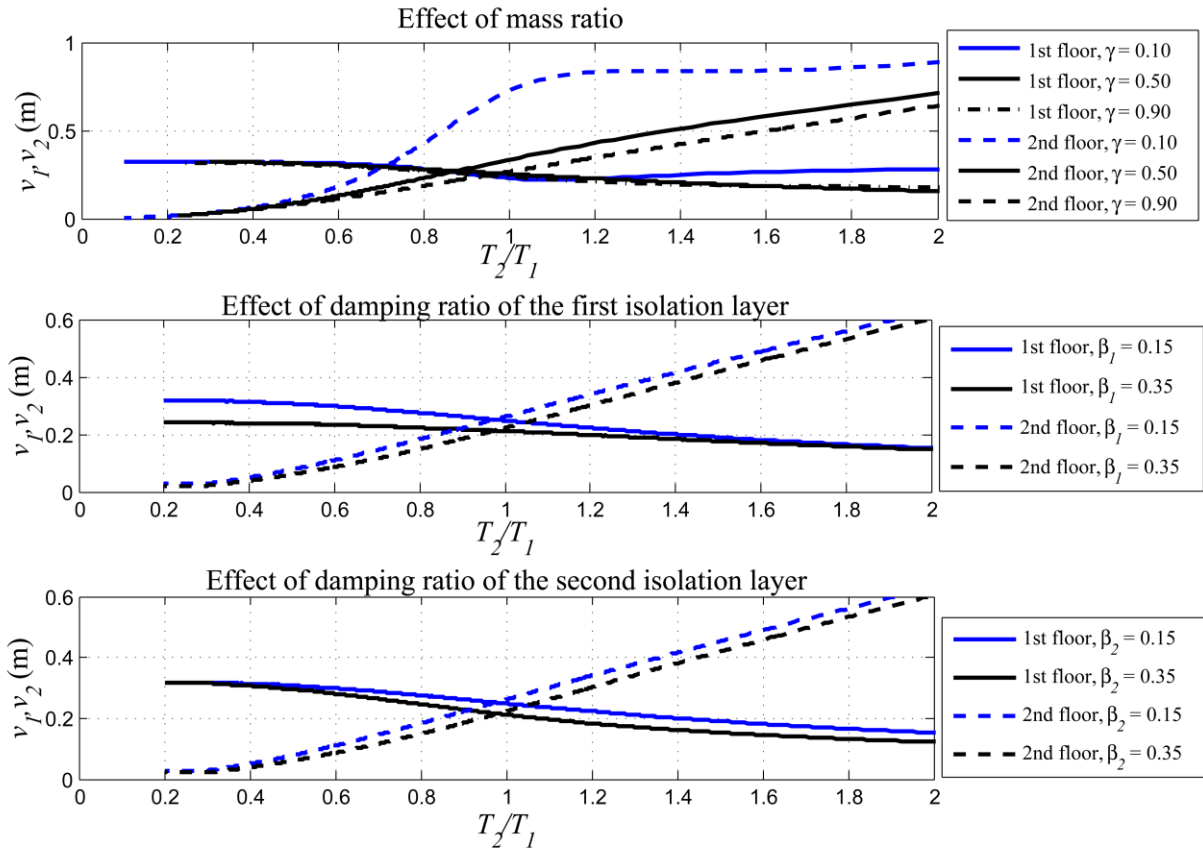


Fig. 2 - Effect of Mass Ratio and Damping Ratios on Dual Isolation System, $T_1=3.5$ s

at 15% and γ is 0.9. Figure 2c varies β_2 , while β_1 is kept at 15% and γ is 0.9. The left side of the graph represents the traditional base isolation system in which the natural period of the first floor is much longer than the second floor. For all scenarios presented, as the period of the second DOF increases, the story drift of the first layer is reduced with the concession of increased lateral displacements in the second layer. As the both the reduction of the first layer as well as the total roof displacement of the building are important, the middle point in which the period of the second floor approaches the period of the first layer is chosen to represent the dual isolation system.

In Fig. 2a, it can be seen that larger mass ratios mitigate the large displacements of the second isolation layer. In effect, this reduces the overall roof displacement, and therefore γ is suggested to be as large as possible. Figure 2b shows that increasing the damping ratio of the first isolation layer results in only minimal reductions of the isolation layer displacement. For example, when γ is 0.9 and β_1 is 15%, the dual isolation system reduces the first floor displacement by 34% from classic base isolation; however, when β_1 is 35% the reduction is only 12% as shown in Fig. 2b. Thus, it is not worth additional costs to increase the damping level in this layer. Figure 2c shows the effect of β_2 on the floor's displacement. Damping in the second isolation has a significantly higher effect on the displacements of both the first and second isolation layers. Larger damping of the second degree of freedom effectively decreases both the first and second DOF's displacement, while the system maintains its efficiency in reducing the total displacement of the building. Based off these results, β_2 is suggested as 35% for the system.

3. Time History Analysis

To evaluate the performance of the dual isolation system compared to classical base isolation a suite of five broadband and five pulse type ground motions, scaled to the DBE spectrum were selected. The ground motions specifications are listed in Table 1. The response spectra of the ground motions are shown in Fig. 3. Based on the analysis of the previous section, the dual isolation system considered for this analysis has a period of 3.5 s and a damping ratio of 15% for the first layer. The upper isolation layer is tuned to the first layer and has a period of 3.5 s and a damping ratio of 35%. A large mass ratio, $\gamma = 0.9$, was selected to further control the roof displacement. If, for example, a ten story building was being designed, a mass ratio of 0.9 could roughly be achieved by placing isolation layers at the base level and in between the first and second stories. For comparison, a classic isolation system is modeled as a SDOF system, with a period of 3.5 s and a damping ratio of 15%.

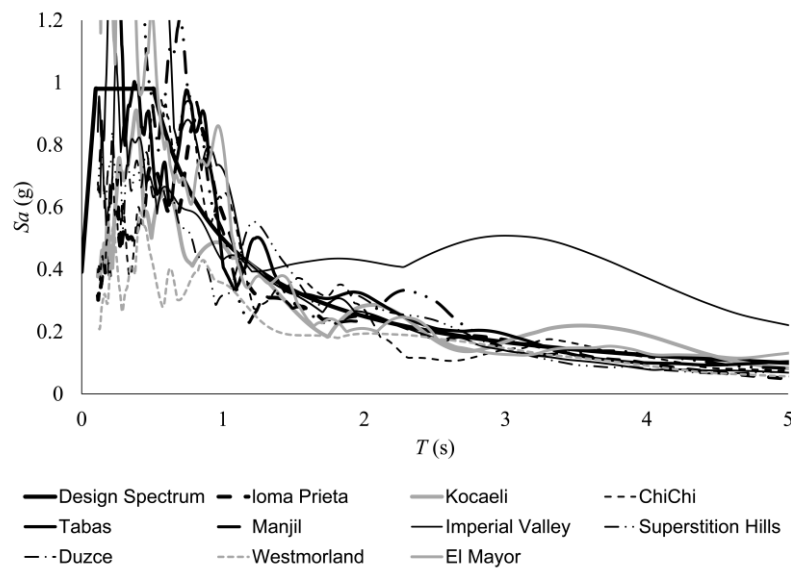


Fig. 3 - Ground Motion Response Spectra

The time history of the floor acceleration and displacement responses of the dual isolation and classic isolation are shown in Fig. 4 for Westmorland and Manjil. In addition, the peak displacement and acceleration responses to seismic excitations are presented in Table 2. The time history analysis results show that the relative displacement of the first DOF of the dual isolation system v_1 , is reduced significantly for both pulse and non-pulse type motions compared to the classic base isolation system, by up to 48%.

Table 1: Selected Ground motions

#	NGA Record #	Earthquake	Year	Station	Scale Factor	Pulse Period
1	778	Loma Prieta	1989	Hollister Diff. Array	1.624	-
2	1158	Kocaeli	1999	Duzce	0.855	-
3	1203	Chi Chi	1999	CHY036	1.35	-
4	1633	Manjil	1990	Abbar	1.475	-
5	5829	El Mayor	2010	RITTO	1.223	-
6	181	Imperial Valley	1979	El Centro Array #6	1.024	2.6
7	316	Westmorland	1981	Parachute Test Site	1.84	3.6
8	721	Superstition Hills	1987	El Centro Emp. Co	1.588	2.4
9	143	Tabas	1978	Tabas	0.584	6.18
10	1602	Duzce	1999	Bolu	0.9518	0.882

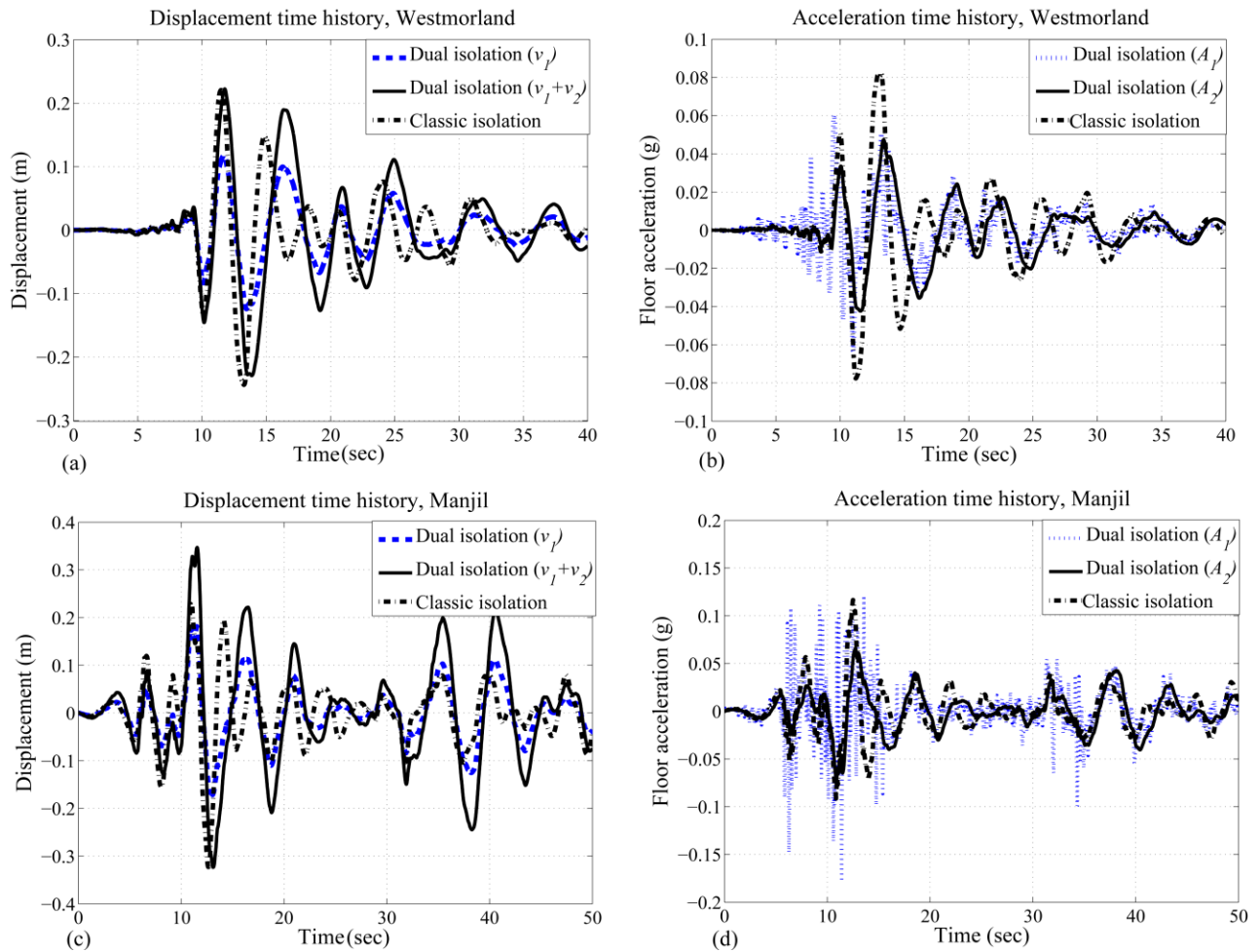


Fig. 4 - Time History Analysis, (a) Displacement (Westmorland), (b) Floor acceleration (Westmorland), (c) Displacement (Manjil), (d) Floor Acceleration (Manjil)

Table 2: Peak Responses to Ground Motions

Ground motion	Classic Isolation		Dual Isolation			
	v_1 (m)	A_1 (g)	v_1 (m)	v_1+v_2 (m)	A_1 (g)	A_2 (g)
Loma Prieta	0.28	0.10	0.16	0.27	0.10	0.06
Kocaeli	0.41	0.13	0.23	0.43	0.10	0.08
Chi Chi	0.24	0.08	0.17	0.36	0.09	0.06
Manjil	0.32	0.12	0.18	0.35	0.18	0.07
El Mayor	0.27	0.10	0.26	0.49	0.12	0.10
Imperial Valley	0.95	0.33	0.57	1.05	0.19	0.20
Westmorland	0.24	0.08	0.13	0.23	0.06	0.04
Superstition Hills	0.23	0.08	0.12	0.24	0.07	0.05
Tabas	0.30	0.11	0.20	0.36	0.13	0.07
Duzce	0.21	0.08	0.14	0.26	0.15	0.05

However, the total displacement of the roof (v_1+v_2) is increased by 19% on average compared to the classic isolation system.

The efficiency of the dual isolation system depends on the frequency content of the ground motion. The dual isolation system is more effective for motions such as Loma Prieta and Westmorland, which have more energy in the lower frequency range, between 0.3 to 1 Hz, close to the frequency of the isolated system. For example, the total displacement at roof level increased by 19% on average for all motions, but increased by only 5% on average for motions with lower frequency content. The dual isolation system is not as effective for motions such as El Mayor and Manjil, which have high frequency content.

In the dual isolation system, the peak acceleration of the second DOF decreases by 35% on average for all motions. The peak acceleration of the first DOF remains almost equal to that of the classic isolation system for ground motions with lower frequency content, whereas the acceleration increases for motions with high frequency content. However, as the second DOF represents approximately 90% of the building (corresponding to the selected mass ratio), a significant reduction in acceleration has been achieved for the majority of the building while the displacement of the first floor has been decreased. This reduction in peak acceleration of the second superstructure increases the protection of acceleration sensitive equipment and non-structural components and provides occupants with increased comfort.

4. Floor Response Spectra and Effect of Higher Modes

4.1. Effect of Higher Modes

This section aims to investigate the effect of higher modes on the linear behaviour of the dual isolation system compared to its classic isolation counterpart. A ten story building with two isolation layers at the base and second floor, following the mass ratio $\gamma = 0.9$, is selected. For this model, the period of the single-story superstructure on top of the first isolation layer is 0.25 s, and the period of the nine-story superstructure on the second isolation layer is 0.9 s. Both superstructures are assigned 5% Rayleigh damping. The nominal periods and damping ratios of the first and second isolation layers is $T_1 = T_2 = 3.5$ s, $\beta_1 = 15\%$, and $\beta_2 = 35\%$ respectively. For comparison, the classic base isolated system consists of an isolation layer ($T = 3.5$ s and $\beta = 15\%$) at the base with a ten story superstructure with fundamental period $T = 1$ s with 5% Rayleigh damping.

The interstory drifts of the classic isolation model compared to the dual isolation model are shown in Fig. 5 for the significant duration of the Westmorland motion. The dual isolation decreases the interstory drifts in both the first and the second superstructures. However, the reduction is significantly larger for the interstory drift of the superstructure on top of the first isolation layer. Figure 6 shows the average distribution of the maximum floor acceleration and interstory drift over the height of the structure. The displacement at the base level of the dual isolation model is decreased by roughly 38%. In addition, roughly 40% reduction in floor acceleration is observed at the second floor (directly above the 2nd isolation layer) and the roof of the dual isolation model.

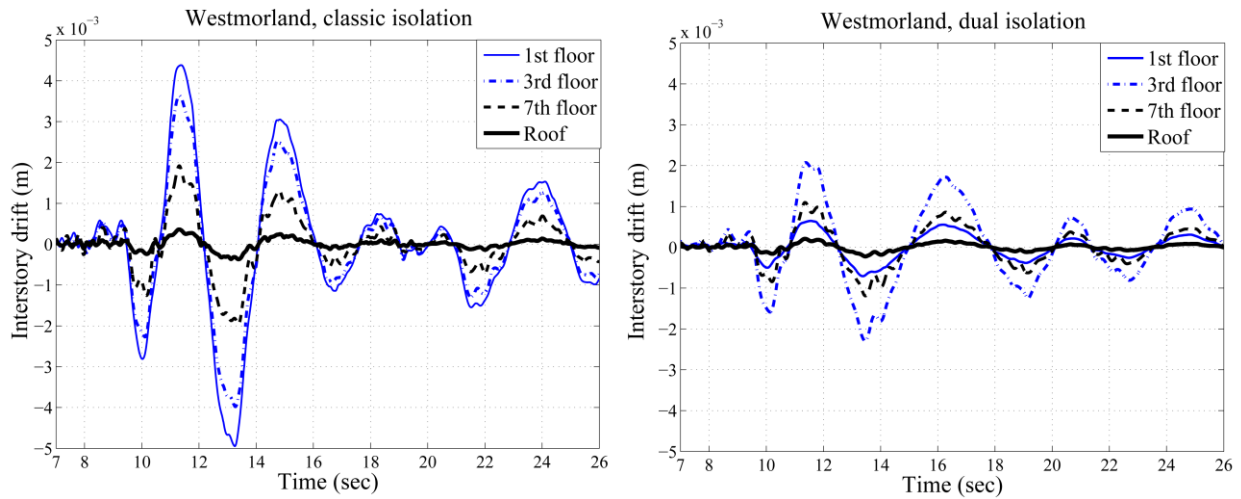


Fig. 5 - Interstory Drift, Westmorland, Left: Classic Isolation, Right: Dual Isolation

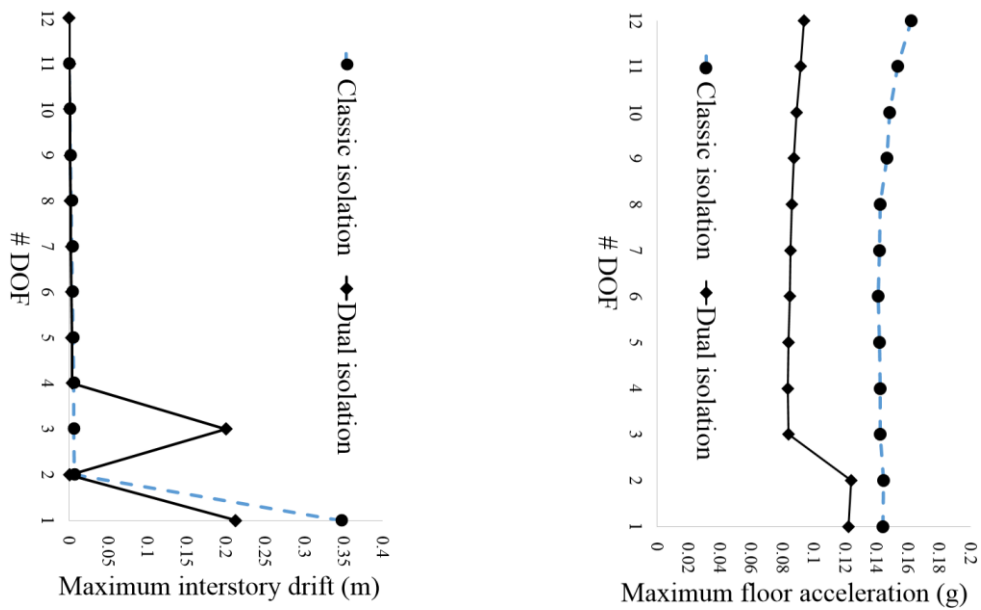


Fig. 6 - Average of Motions, Left: Maximum Interstory Drift, Right: Maximum Floor Acceleration

4.2. Floor Response Spectrum

Floor response spectra reflect the effectiveness of the proposed isolation system in protecting building systems and contents on any particular floor of the building. The spectral accelerations of a secondary system with 5% damping ratio are shown over the period range from 0.05 s to 5 s in Fig. 7. The response spectrum is shown for the 1st floor (directly above the first isolation layer), 3rd floor (above the second isolation layer), and roof for Westmorland and Manjil as an example of ground motions which have low and high frequency content. The demands on contents and systems in the upper portion of the structures are significantly decreased for both motions over the total frequency bandwidth. This finding is in line with the decreased acceleration demand in dual isolation systems as explored in Section 3.

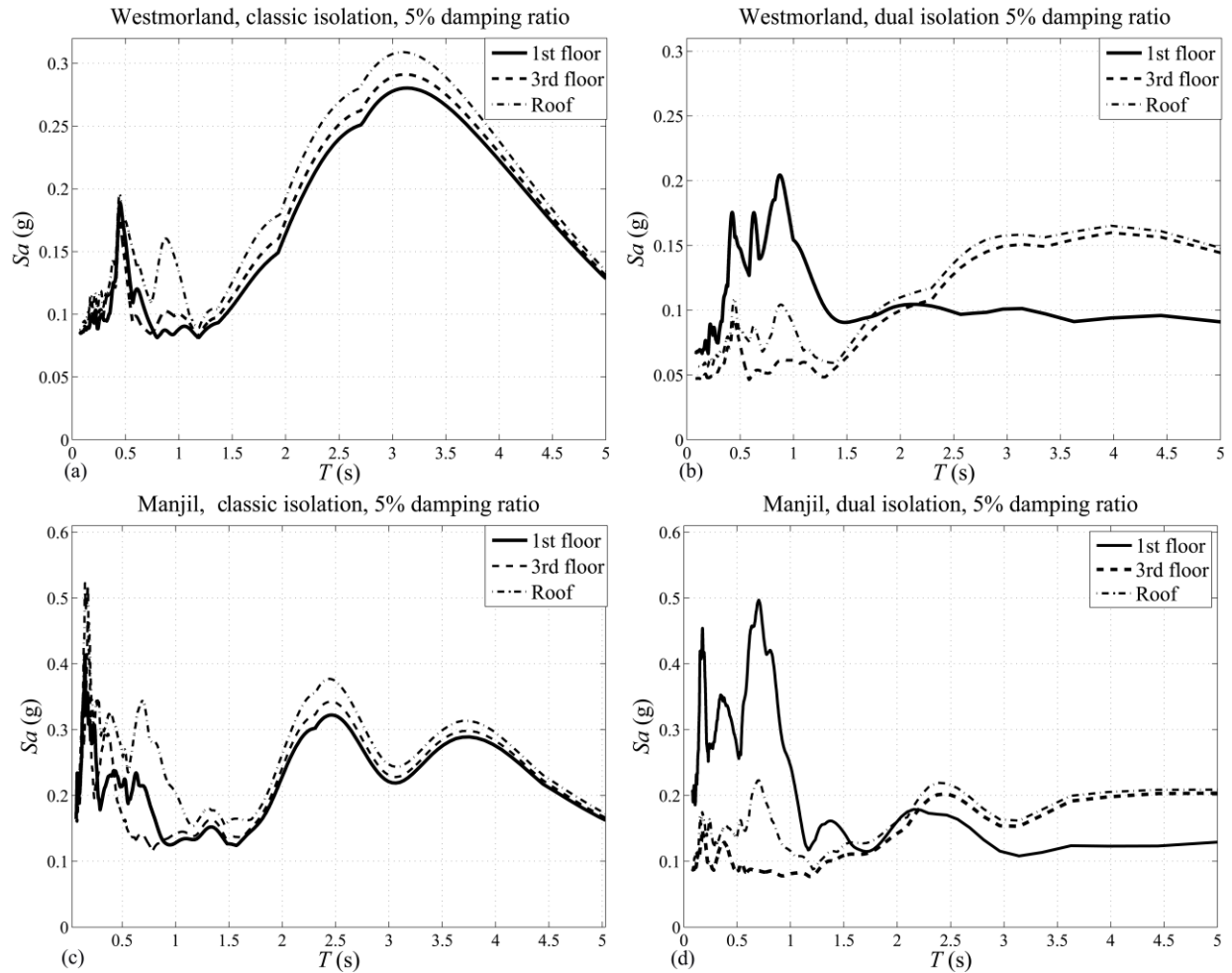


Fig. 7 - Floor Response Spectra, (a) Westmorland, Classic Isolation, (b) Westmorland Dual Isolation, (c) Manjil, Classic Isolation, (d) Manjil, Dual Isolation

The maximum acceleration responses on the first floor are as the same order as the classic isolation model for period range below 0.5 s but increase significantly in the 1 s period range, close to the second period of the dual isolated structure. While the demands are increased for the first floor over a limited range, this represents only 1/10th of the building floor area and thus, a major decrease in demand is seen for the majority of contents. The same trend is observed for both high and low frequency content motions.

5. Conclusion

Presented in this study, the application of an innovative isolation configuration, with two layers of isolation at the base and mid-story is investigated. From response spectrum analysis the ratio of the frequencies of the two isolation systems was selected to be one, and a larger mass ratio γ was found to be beneficial for the reduction of displacements for both degrees of freedom, so a mass ratio of 0.9 was selected. It was shown that a low to moderate damping ratio for the first isolation layer and a larger damping ratio for the second isolation layer improves the displacement behaviour of the system. The system was analyzed under ten scaled ground motions with varying frequency content, including five pulse type records, to investigate story drifts and accelerations. The proposed system is most effective in reducing the displacement and acceleration responses (compared to a classic base isolated building) under excitations with frequency content closer to that of the isolation system, in the 0.3 to 1 Hz range. The adoption of the second isolation layer reduces the lateral displacement of first layer by 37% on average and up to 48% compared to classical base isolation. The roof displacement increased by 19% on average. However, it is

on the same order of the roof displacement of classic isolation systems for ground motions at the optimum frequency range.

Extension of the two DOF model to multi DOF shows decreased interstory drifts in both the first and the second superstructures. An increased demand on building contents below the second isolation layer in 1 s period range close to the second period of the dual isolation system is observed. However, the dual isolation system decreases the peak floor acceleration in the second layer of the superstructure (which represents the majority of the building floor area) by 40% on average compared to its base isolation counterpart. Large reductions are also seen in floor response spectra over the frequency range associated with building systems and components. This reduction increases occupants' safety, reduces the damage to non-structural components and enhances the building's capability to remain fully operational after earthquake.

Designing a dual isolation system will result in an increased number of bearings compared to the classic isolation, as well as increased costs due to architectural and mechanical detailing necessary for mid-story isolation systems. However, bearing sizes and isolation gaps may be reduced for specific applications. As the system offers large reduced demand parameters, it can be used for applications which call for enhanced protection of the building systems and components.

6. References

- ASCE/ SEI 7-10. "Minimum Design Loads for Buildings and Other Structures", *American Society of Civil Engineers*, 2010.
- CHIEN PAN, T., FU LING, S., CUI, W., "Seismic Response of Segmental Buildings". *Journal of Earthquake Engineering and Structural Dynamics*, 24(7), 1995, pp. 1039-1048
- CHOWDHURY, A., IWUCHNKWU, M., GARSKE, J., "The Past and Future of Seismic Effectiveness of Tuned Mass Dampers". *Structural Control*, 1987, pp.105-127.
- CLARK, A. "Multiple Passive Tuned Mass Dampers for Reducing Earthquake Induced Building Motion", *9th World Conference on Earthquake Engineering, Kyoto, Japan*, Vol. V, 1987, pp. 779-784.
- KELLY, J., "The Role of Damping in Seismic Isolation", *Journal of Earthquake Engineering and Structural Dynamics*, 28(1), 1999, pp. 3-20.
- MATTA, E. "Effectiveness of Tuned Mass Dampers Against Ground Motion Pulses", *Journal of Structural Engineering*, 139(2), 2012, pp. 188-198.
- NAEIM, F., KELLY, J. M., "Design of Seismic Isolated Structures". John Wiley and Sons, Inc., 1999.
- PALAZZO, B., PETTI, L. "Combined Control Strategy: Base Isolation and Tuned Mass Damper", *ISET Journal of Earthquake Technology*, 36, 1999, pp. 121-137.
- RYAN, K., EARL, C. "Analysis and Design of Inter-Story Isolation Systems with Nonlinear Devices", *Journal of Earthquake Engineering*, 14 (7), 2010, pp. 1044-1062.
- SLADAK, J., KLINGER, R. "Effect of Tuned-Mass Dampers on Seismic Response", *Journal of Structural Engineering*, 109(8), 1983, pp. 2004-2009.
- TANIGUCHI, T., DER KIUREGHIAN, A., MELKUMYAN, M. "Effect of Tuned Mass Damper on Displacement Demand of Base-Isolated Structures", *Engineering Structures*, 30(12), 2008, pp. 3478-3488.
- WOLFF, E., IPEK, C., CONSTANTINOU, M., TAPAN, M. "Effect of viscous damping devices on the response of seismically isolated structures". *Journal of Earthquake Engineering and Structural Dynamics*, 44 (2), 2015, pp. 185-198.